# Simulation and Theory of Self-Assembled Networks: Ends, Junctions, and Loops†

**James T. Kindt***

*Department of Chemistry and Cherry L. Emerson Center for Scientific Computation, Emory University, Atlanta, Georgia 30322-1003*

*Received: March 11, 2002; In Final Form: June 4, 2002*

The equilibrium assembly of chains capable of forming 3-fold junctions, a phenomenon observed in wormlike micelles, microemulsions, and ferromagnetic colloids, is studied by mean-field theory and Monte Carlo simulation. First, the theoretical description formulated by Tlusty and Safran (*Science* **2000**, *290*, 1328) is revisited by treating junctions as the product of end-interior binary interactions rather than the ternary association of chain ends. Although the final results are equivalent, a new perspective is gained in which the gas−liquid transition is easily interpreted as a conventional condensation driven by explicit attractions. Grand canonical Monte Carlo simulation results on a model of hard spheres self-assembling into semiflexible chains with 3-fold junctions are in qualitative agreement with mean-field theory. In contrast, in a flexible model with equivalent chaining and junction association constants, the expected gas−liquid transition is apparently suppressed by the presence of loops, the products of intrachain junction formation. The effects of loop formation on the phase diagram are explored using a simple extension of the mean-field theory.

## I. Introduction

The reversibly self-assembled aggregates of molecules, macromolecules, and colloidal particles are useful both as "soft" materials responsive to their environment and as templates of tunable structure for the synthesis of more permanent materials.[1] One of the simplest types of self-assembly is equilibrium polymerization, characterized by aggregates that can reversibly grow to arbitrary length while maintaining a fixed thickness. It is well-known that ideal equilibrium polymer system models, those in which interactions between aggregates are neglected, do not exhibit a first-order phase transition.[2] A common real-world complication to this ideal picture is that systems which favor one-dimensional growth, such as wormlike micelles and dipolar colloidal suspensions, may also exhibit branch-points or junctions. The presence of occasional junctions along the chain structure has dramatic effects on the structure, dynamics, and thermodynamics of the self-assembled system, which may include the appearance of a first-order phase transition and/or a percolation transition to an extended network structure.

The theory of the thermodynamics of self-assembled network has been developed by Tlusty and Safran[3] to explain the simulation results of Camp, Shelley, and Patey,[4] who were the first to provide evidence for a gas−liquid transition in dipolar fluids with no additional isotropic attractions. The simulation and theory results together represent the culmination of a decades-long discussion of the presence or absence of this transition in dipolar systems.[5,6] Early simulation results[7] showed particles self-assembled into chains, with dipole vectors running roughly parallel to the chain contour, under conditions where earlier theory[8] predicted a gas−liquid coexistence. This observation contributed to speculation that, like the ideal equilibrium polymer system, fluids with purely dipolar interactions lack a gas−liquid transition.[9] A key insight of Tlusty and Safran (TS) was that while the net electro- or magnetostatic interaction of the interiors of dipolar chains is weak, chain *ends* may interact significantly at short range to form Y-shaped 3-fold junctions, leading to a junction-mediated gas−liquid transition.[3] This insight allowed methods developed to describe microemulsion networks[10] to be applied to dipolar fluid systems. Further investigations of the thermodynamics, and corrections to the mean-field view of the structure of dense networks, have been continued by Zilman and Safran.[11]

In describing the scaling of junction concentration, TS note that their result can be inferred from the equilibrium of the fusion of three chain ends. Here, we use a different approach, which treats first the assembly of chains and then the reversible attachment of chain ends to chain interiors to form 3-fold junctions. The phase transition predicted using this model is equivalent to that of Safran and co-workers,[3,11] but the different set of definitions used simplifies somewhat the interpretation and facilitates the approximate treatment of loop effects.

To further explore the predictions of the theory, a new Monte Carlo simulation technique is applied to investigate the phase behavior of a simple network-forming hard sphere model, and in particular to determine the influence of chain flexibility and intrachain loops. Apart from the dipolar sphere simulations,[4,12] in which long-ranged electro- or magnetostatic interactions among particles in all chains play a role that is not well understood, there have been few simulation efforts on self-assembled networks of this type. (Networks of fixed-length polymers that cross-link reversibly[13] or end-link irreversibly[14] have been subjects of recent simulations.) The potential models used have been of the "associating fluid" type, that is, spheres with short-ranged zones for bonding arranged around them, generally with four sites suggestive of the hydrogen bonds formed by the water molecule.[15] Biased Monte Carlo methods have been devised for more efficient sampling of the bonded structures allowed by these models.[16] The model and technique used in the current study take both of these concepts to their limits: here all bond-lengths are exactly fixed, eliminating a

† Part of the special issue "John C. Tully Festschrift".

* To whom correspondence should be addressed. E-mail: jkindt@emory.edu.

10.1021/jp020670m CCC: $22.00 
Published on Web 07/09/2002

structurally and thermodynamically uninteresting degree of freedom for each bonded particle, and biased Monte Carlo moves are therefore indispensable to add and remove particles to and from the bonding regions, which are of vanishing volume. The grand canonical ensemble is used, allowing biased chain growth, shrinking, and re-growth to sample different conformations. A novel scheme for reversible formation of junctions has been devised, relying on directed monomer addition moves to bridge chain ends and interior monomers. The advantage of this approach is the level of control allowed in the specification of the number, energy, and geometries of permissible bonding structures. In this study, two systems with closely matched free energies of chaining and junction formation but significantly different persistence length are investigated to uncover effects of chain flexibility not treated by the mean-field theory.

## II. Theoretical Background and Simulation Methods

**A. Mean-Field Theory.** To treat the thermodynamics of self-assembly with junctions, a formalism based on the Flory−Huggins theory, previously applied to semiflexible equilibrium polymers with isotropic attractions,[17] was applied and extended. The model for a pure equilibrium polymer system (that is, exhibiting one-dimensional self-assembly, without junctions) in the isotropic phase is first reviewed. The system is assumed to consist of monomers of unit diameter that can each form up to two bonds, with free energy of bonding $U_b^*$ incorporating both the bond energy and the entropy associated with the stretching and bending degrees of freedom. The value of $U_b^*$ is assumed independent of the presence of any other bonds. Through these bonds, monomers reversibly associate into chains of arbitrary integer length. The total number density of all monomers is denoted $\varphi$; the number density of chains of length $i$ is $\varphi_i$. The average chainlength $M$ is defined as the inverse of the number of independent chains (including chains of length one) multiplied by the total monomer concentration

$$M = \varphi(\sum_{i=1} \varphi_i)^{-1} \tag{1}$$

The total number density of ends (where a free monomer, with two free bonding sites, is counted as having two ends), or twice the number density of all chains, is given by

$$\varphi_{\text{end}} = 2\sum_{i=1} \varphi_i = 2\varphi M^{-1} \tag{2}$$

Similarly, the total number density of bonds equals $\varphi(1 - M^{-1})$. These are both independent of the precise distribution of chain lengths. The total free energy density of the system consists of the translational entropies of all chains in the mixture, the free energy of packing due to excluded volume repulsions, and the internal free energies of all chains. The same form as in the standard treatment of Flory−Huggins theory[18] are used for the first two terms, while the third is simply the product of the concentration of bonds with the bond free energy

$$f_{\text{trans}} + f_{\text{packing}} + f_{\text{bond}} = kT\sum_i \varphi_i(\ln\varphi_i - 1) + kT(1 - \varphi)[\ln(1 - \varphi) - 1] - U_b^*(1 - M^{-1})\varphi \tag{3}$$

Minimization of this term over all possible length distributions at fixed $M$ and $\varphi$ gives an exponential distribution of concentrations of chains as a function of chainlength $i$, with $\varphi_i$ proportional to $(1 - M^{-1})^i$, yielding an overall free energy

$$f_{\text{chains}} = kT\frac{\varphi}{M}\left[\ln\frac{\varphi}{M^2} - 1\right] + kT(1 - \varphi)[\ln(1 - \varphi) - 1] - U_b^*(1 - M^{-1})\varphi + kT\varphi(1 - M^{-1})\ln(1 - M^{-1}) \tag{4}$$

The free-energetic minimum average chainlength for ideal, chain-only system is

$$M = \frac{1}{2} + \frac{1}{2}\sqrt{1 + 4\varphi \exp(\beta U_b^*)} \tag{5}$$

We now consider the association of chains at junctions as a formal second step in self-assembly. One way to describe a junction is as a bonding interaction shared by three ends, reducing the large defect energy of a chain termination to a smaller, junction energy. We will use an equally valid definition, in which a junction is defined as an association between the end of a chain and the interior of another (or possibly the same) chain, releasing an energy $U_T$. (In the "defect" vocabulary of Safran et al., which takes an unbroken unbranched chain as the ground-state rather than a gas of free monomers, the end energy $\epsilon_1$ and the junction energy $\epsilon_3$ correspond to $U_b/2$ and $U_b/2 - U_T$ respectively.) Note that the definition of what constitutes a chain may differ in the two pictures; in the present construction, a junction formed in the middle of a chain does not alter the chain length. Given the free energy of the self-assembled system of chains of average length $M$ in the absence of junctions, one can calculate through a mean-field approximation the free energy change in the system when end-interior junctions are allowed to form. Consider the chain-only system at a given $M$ and $\varphi$, and $T$. The free energy density change upon introducing junctions, in the mean-field limit where correlations between chains are not explicitly accounted for, is the free energy change per chain multiplied by the concentration of chains. For each chain (which is considered fixed in its orientation and conformation, these degrees of freedom having been taken into account), two new lower-energy states are added: one end or both ends may terminate in a junction. The single-chain partition function associated with the three states (free, one end, or both end bound) is

$$q_{\text{jn-equil}} = (1 + 2\varphi\alpha_T \exp\beta U_T + \varphi^2\alpha_T{}^2 \exp 2\beta U_T) \tag{6}$$

This expression is obtained by considering the Boltzmann-weighted volume available to a given frozen chain. The contribution from the free state is set to unity, as the translational free energy is already accounted for in the chain-only expression. There are $\varphi = N/V$ binding sites available per unit volume, each of which is assumed to have effective volume $\alpha_T$ to which the position of the chain end is restricted, to which either end of the chain may potentially form a junction. Given the assumption of the uniform distribution of monomers and therefore of binding sites, the volume fraction of chain positions in which *both* ends can form junctions is the square of the volume fraction of binding sites. The partition function associated with allowing each (distinguishable) chain independently to form one or two junctions becomes[19]

$$Q_{\text{jn}} = Q_{\text{ch}}(N,V,T,M)[q(\varphi,T,M)]^{N/M} \tag{7}$$

and the free energy density

$$f_{\text{jn}}(\varphi,T,M) = f_{\text{ch}} - 2kT\frac{\varphi}{M}\ln[1 + \varphi \exp(\beta U_T^*)] \tag{8}$$

where the entropic factor $\alpha_T$ has been folded into a free energy

of junction formation, $-U_T^*$. The mean chainlength $M$ is still well-defined in the system given the formal assumption that exactly one chain terminates at each junction, and has the following dependence on volume fraction and temperature

$$M = \frac{1}{2} + \frac{1}{2}\sqrt{1 + \frac{4\varphi \exp(\beta U_b^*)}{[1 + \varphi \exp(\beta U_T^*)]^2}} \approx \frac{\varphi^{1/2} \exp(\beta U_b^*/2)}{1 + \varphi \exp(\beta U_T^*)} \quad (9)$$

The second expression represents the highly polymerized limit $M \gg 1$. The numerator gives the square-root dependence of mean chainlength on concentration for an equilibrium polymer system in the absence of junctions. Deviation from this scaling becomes significant when $\varphi$ approaches $\exp(-\beta U_T^*)$; the function passes through a maximum at $\varphi = \exp(-\beta U_T^*)$.

Considering this same limit of $M \gg 1$, the total free energy from eqs 4 and 8 can be rewritten as follows

$$f_{jn} = kT\frac{\varphi}{M}\left\{\ln\frac{\varphi}{M^2} - 2 + U_b^* - 2\ln[1 + \varphi \exp(\beta U_T^*)]\right\} + kT(1 - \varphi)[\ln(1 - \varphi) - 1] - U_b^*\varphi \quad (10)$$

Upon substitution of the limiting expression for $M$ from eq 6, removing all terms that scale linearly with $\varphi$ (and therefore do not affect the phase behavior) and taking the low-$\varphi$ limit of the steric repulsion term, this expression gives a result of identical form to eq 2 of ref 3

$$f_{jn} = -2kT\varphi^{1/2} \exp(-\beta U_b^*/2) - 2kT\varphi^{3/2} \exp[\beta(-U_b^*/2 + U_T^*)] + kT\varphi^2 \quad (11)$$

This confirms that the present approach is equivalent to the theory of Tlusty and Safran, with the substitutions of $U_b/2$ and $U_b/2$-$U_T$ for their end energy $\epsilon_1$ and junction energy $\epsilon_3$ respectively. The same $\varphi^{3/2}$ scaling of the junction contribution to free energy is obtained either from the equilibrium association of three chain ends [ $(\varphi^{1/2})^3$, where the end concentration $\propto\varphi^{1/2}$ ] or from the association of chain end with chain interior $[(\varphi^{1/2})\varphi]$.

For the calculation of phase coexistence curves, the chemical potential of the system is obtained by taking the derivative of eq 8 with respect to $\varphi$

$$\beta\mu_{juncs} = -\ln(1 - \varphi) + \ln\left(\frac{\varphi}{M^2}\right) + (1 - M^{-1})\ln(1 - M^{-1}) - (1 - M^{-1})\beta U_b^* - 2M^{-1}\ln[1 + \varphi \exp(\beta U_T^*)] - \{2M^{-1}\varphi \exp(\beta U_T^*)\}/\{[1 + \varphi \exp(\beta U_T^*)]\} \quad (12)$$

where $M$ is given the optimum value of eq 9. Phase coexistence curves were calculated by numerical search for $\varphi_{gas}$ and $\varphi_{liquid}$ satisfying

$$\mu(\varphi_{gas}) = \mu(\varphi_{liquid}) = \frac{f(\varphi_{liquid}) - f(\varphi_{gas})}{\varphi_{liquid} - \varphi_{gas}} \quad (13)$$

**B. Grand Canonical Monte Carlo Simulation Methods.** Monte Carlo simulations were performed in the grand canonical ensemble (constant $\mu,V,T$, with $\mu$ the chemical potential) to evaluate phase transitions without involving volume-change moves, which are likely to be inefficient for percolated networked structures. In the model employed, all particles experience hard-sphere excluded-volume interactions with all other particles; the sphere diameter is defined as unity. Bonded particles are kept at a distance of exactly 1.0; acceptance probabilities were calculated as though a square-well potential surrounded each particle between $r = 1.0$ and $r = 1.0 + \Delta$, in the limit $\Delta \to 0$. The full potential applies for up to two bonds per particle, with the restriction that the angle formed by any triplet of connected particles must be greater than $\theta_{min}$. Any particle on the interior of a chain (that is, already bound to two others) may become a junction by binding a third particle. Although no additional angle restriction applies to the third particle, at least one pair of bonds to the junction particle must form an angle greater than $\theta_{min}$. The energy released upon forming a bond is $U_{ch}$, except for the third bond to a junction, which has the lower energy $U_j$.

In the Monte Carlo scheme employed, all chain growth is achieved through directed addition and all junction formation is achieved through directed bridging additions between ends (or free monomers) and chain interior monomers. Chain conformations fluctuate only through shrinking and re-growth. This method is well suited for the present investigation of the end-junction transition, but is not appropriate for simulation of networks in the limit where no free ends are available. Five types of Monte Carlo moves are employed. The first two are standard for GCMC: with 5% probability each, a free monomer is added to or removed from the system, with acceptance probabilities[20]

$$\mathrm{acc}(N_{free} \to N_{free} + 1) = \min\left[1, \frac{V}{N_{free} + 1} \exp(\beta\mu)\right] \quad (14)$$

and

$$\mathrm{acc}(N_{free} \to N_{free} - 1) = \min\left[1, \frac{N_{free}}{V} \exp(-\beta\mu)\right] \quad (15)$$

where the thermal de Broglie wavelength is has been set equal to unity. No bonds may be formed or broken during this step, so the change in energy is zero (except for insertion moves to positions that overlap existing particles, which are rejected).

Otherwise, with equal (30%) probabilities, a directed addition to a monomer or chain end is attempted, a particle is attempted to be removed from an end, or a particle is attempted to be removed from a junction. As explained below, the directed addition move may either result in the extension of a chain or, if the original trial position overlaps a suitable monomer in the interior of a chain, a bridging addition that forms a junction. The directed addition move requires that a lists of all unbonded particles and all chain ends be maintained; the total number of monomers and chain ends represents the number of available sites for chain extension moves, and is called $N_{avail}$. One of these, either a free monomer, or a chain end, is selected with uniform probability. A position at a distance 1.0 from the particle is selected for the trial position of the new particle. If the particle to be added to is a free monomer, the vector between the particle and the monomer is chosen from the unit sphere. Otherwise, the position is chosen from the truncated part of the unit sphere that satisfies the minimum bond angle requirement. The volume of possible positions is $4\pi\Delta$ for dimerization (i.e., addition to a monomer), and $2\pi\Delta(1+\cos\theta_{min})$ for chain extension. If the position does not overlap existing spheres, the move is accepted with a probability

$$\mathrm{acc}_{end-addition} = \min[1, 2\pi\Delta(1 + \cos\theta_{min}) \exp(\beta\mu + \beta U_{ch})] \quad (16)$$

for addition to a chain end, and

$$\mathrm{acc}_{\mathrm{dimer}} = \min\left[1, N_{\mathrm{avail}}(N_{\mathrm{avail}}+1)^{-1} 4\pi\Delta \exp(\beta\mu + \beta U_{\mathrm{ch}})\right] \quad (17)$$

for addition to a monomer. The vanishing shell thickness $\Delta$ always appears in conjunction with the Boltzmann factor for formation of a bond, so a free energy of chain extension $U^*_{\mathrm{ch}}$ may be defined as

$$U^*_{\mathrm{ch}} = U_{\mathrm{ch}} + kT\ln(4\pi\Delta) \quad (18)$$

The relationship between the energy $U^*_{\mathrm{ch}}$ defined here and the energy $U^*_{\mathrm{b}}$ that enters the mean-field theory is discussed in the section IIC, below. The acceptance probabilities for the reverse moves are

$$\mathrm{acc}_{\text{chain end}-\text{removal}} = \min\left[1, 2(1+\cos\theta_{\mathrm{min}})^{-1} \exp(-\beta\mu - \beta U^*_{\mathrm{ch}})\right] \quad (19)$$

and

$$\mathrm{acc}_{\text{dimer end}-\text{removal}} = \min\left[1, N_{\mathrm{avail}}(N_{\mathrm{avail}}-1)^{-1} \exp(-\beta\mu - \beta U^*_{\mathrm{ch}})\right] \quad (20)$$

If the trial position overlaps an existing particle, formation of a junction is attempted. As the position may overlap more than one existing particle, all overlaps must be identified. Potential junction targets must be at a distance $d$ greater than $(2 + 2\cos\theta_{\mathrm{min}})^{1/2}$ from the particle being added onto, must have exactly two bonds already, and cannot be bonded to a junction. (This ensures a spacing of at least one monomer between any two junctions, which simplifies bookkeeping and is consistent with the picture that junctions connect chains, not monomers.) One of the $n$ possible candidates is selected at random. A position on the circle equidistant between the existing chain end or monomer and the potential junction, formed by the intersection of the unit spheres centered at these two particles, is selected at random. The region to which the particle is added is, in the limit of small $\Delta$, the structure formed from the rotation of a parallelogram of area $(d\sqrt{1-0.25d^2})^{-1}\Delta^2$ about the axis connecting the two particles. As the radius of rotation equals $\sqrt{1-0.25d^2}$, the volume from which a position is selected is $2\pi\Delta^2 d^{-1}$. If a chain is being extended, the bond angle formed by the new position with vertex at the original chain end is checked. If it satisfies the bond angle restrictions, the junction is formed with a probability

$$\mathrm{acc}_{\text{junction forming}} = \min\left[1, 2\pi\Delta^2 d^{-1} N_{\mathrm{avail}}(3N_{\mathrm{j}}+3)^{-1} \exp(\beta\mu + \beta U_{\mathrm{ch}} + \beta U_{\mathrm{j}})\right] \quad (21)$$

where $N_{\mathrm{j}}$ is the number of existing junctions in the system. Again, it is desirable to remove $\Delta$ from the expression by defining a junction-forming free energy

$$U^*_{\mathrm{j}} = U_{\mathrm{j}} + kT\ln(\Delta/2) \quad (22)$$

to rewrite eq 21 as

$$\mathrm{acc}_{\text{junction forming}} = \min\left[1, d^{-}N_{\mathrm{avail}}(3N_{\mathrm{j}}+3)^{-1} \exp(\beta\mu + \beta U^*_{\mathrm{ch}} + \beta U^*_{\mathrm{j}})\right] \quad (23)$$

The relationship between $U^*_{\mathrm{j}}$ and the free energy of junction formation $U^*_T$ used in the mean-field theory is clarified in section IIC. Equation 23 also applies to junctions formed by bridging a free monomer with a potential junction site; in both cases the volume associated with the directed addition is the same.

In the reverse move, which is attempted in 30% of all moves, a particle attached to a junction is selected at random. For it to be removed, it also must be attached to one other particle that is not a junction, and the remaining particles bound to the junction must satisfy the bond angle restriction. Because the probability of proposing a given junction in the first place depends on the angle-restricted overlaps of several particles, it is difficult to calculate analytically; to maintain detailed balance during the reverse move, a trial ghost particle is generated from the particle to be left behind, and the removal is allowed to proceed only if the generated particle overlaps the same, junction particle. (The idea, the same as that used in configuration bias Monte Carlo, is to use a Monte Carlo method to account for the probability of proposing a given move when a reversal of that move is attempted.[20]) The number $n$ of possible candidates for the ghost particle is evaluated (keeping in mind that particles bound to the junction particle would be possible candidates before the junction is formed), and the removal step is accepted with a probability

$$\mathrm{acc}_{\text{junction break}} = \min\left[1, 3N_j d n^{-1}(N_{\mathrm{avail}}+1)^{-1} \exp(-\beta\mu - \beta U^*_{\mathrm{ch}} - \beta U^*_{\mathrm{j}})\right] \quad (24)$$

When a free monomer instead of a free chain end is left by the junction breaking move, $(N_{\mathrm{avail}})^{-1}$ is substituted for $(N_{\mathrm{avail}}+1)^{-1}$ in eq 24.

To summarize the Monte Carlo scheme for junction formation and breaking, junctions may be formed only by the bridging of a free chain end (or free monomer) by an added particle, which is attempted whenever a chain extension move leads to overlap with an allowed junction site. The advantage of this method is that it does not require monitoring of all possible sites for junctions; any such site will potentially be "discovered" as chains grow and re-grow, in a natural way. An additional choice of move would be the initiation or "budding" of branches off existing chain sites. Use of such a move might improve sampling efficiency; on its own, however, it is incapable of generating segments that terminate with junctions on both ends, and was omitted for the sake of simplicity.

Simulations were performed to obtain $\mu$-$\varphi$ (where $\varphi$ is the total monomer density) isotherms at four temperatures for two systems of differing chain flexibility. The more rigid, referred to as the "semiflexible" system was given a minimum bond angle $\theta_{\mathrm{min}}$ of 2.5 rad (the arc-cosine of $-0.8$, corresponding to a persistence length $l_{\mathrm{p}}$ of 10 bond lengths). In the flexible system, $\theta_{\mathrm{min}}$ was set to $\pi/2$ ($l_p \approx 4$).

At least $10^9$ MC moves were performed for each data point, after an equilibration period of $10^7$ MC moves (or as long as it took for $\rho$ to reach a stable range). Volumes were typically chosen such that $N$ was in the range between 300 and 1500 particles, although for the dense phases at the highest and lowest temperatures studied, larger volumes were chosen to accommodate large observed fluctuations. Coexistence regions were identified by scanning over a range of $\mu$ at a given temperature and looking for discontinuities and hysteresis in the $\mu - \varphi$ isotherm. While more rigorous histogram-reweighting techniques are available to determine coexistence curves,[21] these

rely on generating $\mu - \varphi$ isotherms over temperature points that are much more closely spaced than the present ones; the qualitative shape of the phase diagram is evident from the present method, even if the values of the density at coexistence are not known precisely. As with any finite-size simulation, long-wavelength fluctuations that govern phase behavior near the critical point are not treated properly, and results near the critical point − whose general vicinity is marked by large fluctuations in $\varphi$ at constant $\mu$ − are not expected to be accurate.

**C. Matching Parameters Between Simulation and Theory.** It is desirable to be able to compare simulation and theory as closely as possible, and in particular to be able to match parameters across systems that the theory treats as indistinguishable in order to look for interesting differences in simulation. At a given temperature, two parameters enter the mean-field theory: the equilibrium constant for the end-end association of chains, and the equilibrium constant for the formation of a junction from an end and an interior monomer. These correspond to $\exp(-\beta U_b^*)$ and $\exp(-\beta U_T^*)$, respectively. The relative energetic and entropic contributions to $U_b^*$ and $U_T^*$ determine how these change with temperature, but only their combination enters into the free energy at fixed temperature.

With the present simulation model, monomers are treated as though they are isotropic until they form a bond. This assumption is manifest, for example, through the greater acceptance probability in the directed addition to a free monomer (eq 17) than to a chain end (eq 16). Although this assumption is unimportant in the regime of interest, where free monomers are uncommon compared to monomers in chains, it is noted here to make the point that the equilibrium constant for the extension of a chain by a monomer is not identical to the equilibrium constant for the end-end association of two chains. (Even though chain extension by monomers is the only one explicitly involved in the MC simulation, the latter equilibrium constant is still well-defined and relevant to the theory.) The equilibrium constant for association of a monomer with a chain end is $(1 + \cos\theta_{min})\exp(\beta U_{ch}^*)/2$, by eq 16; this takes into account the restrictions on the bond angle formed. During association of two existing chains, *two* bond angles are formed (both of which share the new bond), yielding a lower equilibrium constant $(1 + \cos\theta_{min})^2\exp(\beta U_{ch}^*)/4$. Therefore, $\exp(\beta U_b^*)$ is equivalent to $(1 + \cos\theta_{min})^2\exp(\beta U_{ch}^*)/4$, or

$$U_b^* = U_{ch}^* + 2k_BT\ln[(1 + \cos\theta_{min})/2] \qquad (25)$$

Several factors enter into the equilibrium constant for junction formation. In a junction formed by the association of a chain end with the interior of another chain, the energy of association is $U_j$. The first entropic factor is the volume of the potential positions around the junction particle at which the chain end can be bound, or $4\pi\Delta$. This is reduced by hard-sphere overlaps with the monomers already bound to the junction. A further complication is that some junction configurations (those in which two or all three bond pairs satisfy the minimum-angle requirement) may break at more than one bond and still leave an allowable bond angle at the junction; this decreases the equilibrium constant for formation of that junction by a factor of 2 or three. The total volume available for the third particle was found by integrating over all positions available to the third particle over the allowed range of bond angles for the preexisting two bonds, taking into account the excluded volume from the three preexisting particles. This was multiplied by the average over all junction configurations of the inverse of the number of breakable bonds. The results, the weighted fraction of the spherical shell around the junction monomer accessible to the incoming end, are $\alpha_1 = 0.66$ at $\theta_{min} = 2.498$ and $\alpha_1 = 0.34$ at $\theta_{min} = \pi/2$. (The latter is lower because of the higher average number of allowable ways to dissociate.)

**TABLE 1: Simulation Input and Correspondence to Theory Input**

| system | $k_BT$[a] | $\exp(\beta U_{ch}^*)$[b] | $\exp(\beta U_j^*)$[c] | $\exp(\beta U_b^*)$[d] | $\exp(\beta U_T^*)$[e] |
|---|---|---|---|---|---|
| $\theta_{min} = 2.5$[f] | | | | | |
| | 0.167 | 40 000 | 50 | 400 | 83 |
| | 0.121 | 400 000 | 75 | 4000 | 124 |
| | 0.094 | $4 \times 10^6$ | 112.5 | 40 000 | 187 |
| | 0.078 | $4 \times 10^7$ | 168.75 | 400 000 | 280 |
| $\theta_{min} = \pi/2$[g] | | | | | |
| | 0.167 | 1600 | 20 | 400 | 85 |
| | 0.121 | 16 000 | 30 | 4000 | 128 |
| | 0.094 | 160 000 | 45 | 40 000 | 192 |
| | 0.078 | $1.6 \times 10^6$ | 67.5 | 400 000 | 288 |

[a] Units of the chain bonding energy. [b] Simulation parameters, as used in eqs 18−24. [c] Simulation parameters, as used in eqs 22−24. [d] As used in eqs 3−12, calculated from simulation parameters by eq 25. [e] As used in eqs 8−12, calculated by eq 26. [f] Effective parameters are $\alpha_b = 1.0$, $U_b = 1.0$, $\alpha_T = 28.2$, $U_T = 0.18$. [g] Effective parameters are $\alpha_b = 1.0$, $U_b = 1.0$, $\alpha_T = 29.0$, $U_T = 0.18$.

Finally, the orientation of the terminal bond of the chain end (or, equivalently, the position of new second nearest neighbor to the junction) is restricted by a factor of $\alpha_2 = (1 + \cos\theta_{min})/2$, as the bond angle restrictions also apply to the new angle formed with vertex at the incoming chain end. Ultimately, the correspondence between the mean-field free energy of junction formation, $U_T^*$, and the factor $U_j^*$ used in the Monte Carlo acceptance probabilities is given by

$$U_T^* = U_j^* + kT\ln[4\pi\alpha_1(1 + \cos\theta_{min})] \qquad (26)$$

Using eqs 25 and 26, values of $U_{ch}^*$ and $U_j^*$ were chosen to yield matched values of $U_T^*$ and $U_b^*$ in the flexible and semiflexible systems, as summarized in Table 1.

## III. Results and Discussion

**A. Mean-Field Theory.** The mean-field statistical thermodynamic theory of self-assembled networks presented above provides a complementary framework to that of Tlusty and Safran.[3] Phase coexistence regions calculated using the free energy of eq 8 have the same inverted teardrop shape (Figure 1, solid curve) as reported previously, at least when the junction-forming energy (an attractive energy, in the present perspective) is lower in magnitude than twice the chain bond energy. At higher junction energies, the system can no longer be described as an equilibrium polymer, as its energetic ground state is a dense network of junctions.

The difference between the theories is only a question of approach and definitions, but one that yields different physical insights. Framing the problem in terms of junctions formed by "sticky" chain ends attracted to interior sites emphasizes the similarities of the transition to more familiar gas−liquid condensations. As the temperature drops, longer and longer chains are formed at lower and lower concentration. The increase in size of the chains diminishes the translational entropy of the system to the extent that the phase transition is complete at low concentration, as in the Flory−Huggins theory of long fixed-length self-attracting polymers near the critical point.[18] Unlike the case of self-assembling polymers condensing due to isotropic attractions,[17] in the network-forming case the mean chain length $M$ is nearly unchanged across the transition, differing by under 3% between coexisting phases for the system represented in

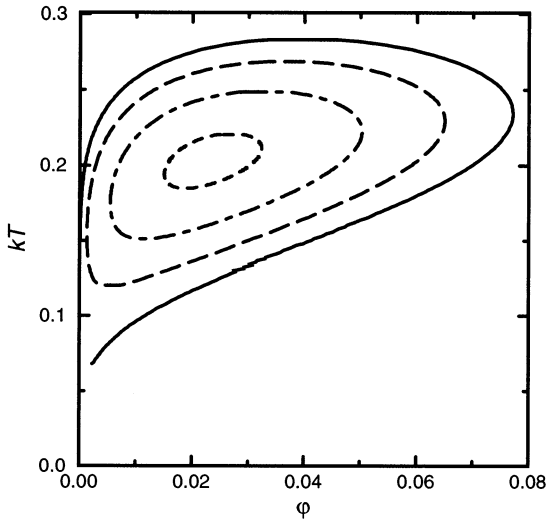


**Figure 1.** Phase coexistence curves calculated from mean-field free energy (solid curve) and free energy corrected for loops (dashed curves). Model parameters are $\alpha_b = 1.0$, $U_b = 1.33$, $\alpha_T = 0.5$, $U_T = 0.55$, chosen to match the corresponding figure in Ref. 3. Solid curve: $\varphi_{intra}$=0.0 (original theory); long-dashed curve, $\varphi_{intra} = 0.005$; dot−dash curve, $\varphi_{intra} = 0.01$; short-dashed curve, $\varphi_{intra} = 0.014$.

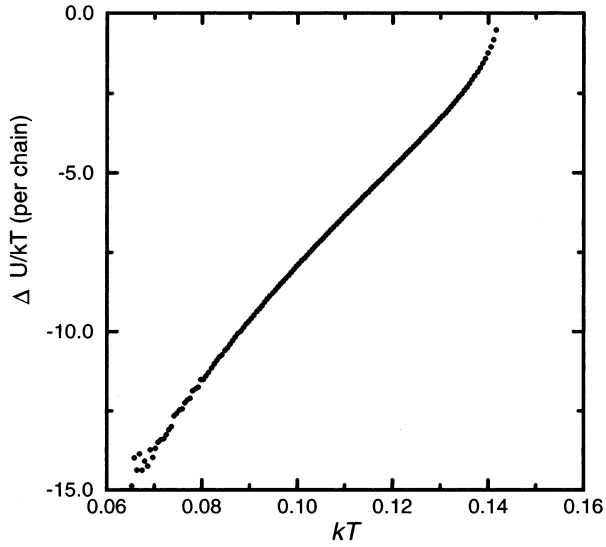


**Figure 2.** Change in mean system energy per chain over gas−liquid transition, from mean-field theory, for system described in Figure 1.

Figure 1. (The mean distance between junctions decreases as more junctions are formed, and in a fully connected network there are on average two internal junctions found along each chain.) Although the energy decrease per monomer is insignificant, the bonding energy released per chain is several times $k_BT$ (Figure 2), in accordance with expectations for gas−liquid transition driven by explicit attractions.

Within the present mean-field theory, as before, equal concentrations of ends and junctions are predicted at the critical point for the gas−liquid transition by mean-field theory (at least in the small-density limit). This condition also marks a lower bound to the onset of extended structural connectivity or percolation, although the percolation transition may occur in the absence of a gas−liquid transition or be completed within the "gas" phase.[11] A feature of the present approach is that it facilitates the treatment of a self-assembling system in which only one end of any given chain is capable of forming a junction. The tree-like, singly connected structures formed in such a system cannot reach percolation except asymptotically, as the number of junctions can never surpass the number of ends. In this case, restriction of the single chain partition function in eq 6 to a single possible bond to be formed leads to the following free energy per unit volume

$$f_{jn,1\ end}(\varphi,T,M) = f_{ch} - kT\frac{\varphi}{M}\ln[1 + \varphi\exp(\beta U_j^*)] \quad (27)$$

whereas the corresponding predicted mean chainlength is

$$M_{jn,1\ end} = \frac{1}{2} + \frac{1}{2}\sqrt{1 + \frac{4\varphi\exp(\beta U_b^*)}{1 + \varphi\exp(\beta U_j^*)}} \approx \sqrt{\frac{\varphi\exp(\beta U_b^*)}{1 + \varphi\exp(\beta U_j^*)}} \quad (28)$$

The free energy of eq 27 does not yield a gas−liquid transition for $U_b^* > U_j^*$, and the mean chainlength of eq 28 has no maximum. It is intriguing that prevention of percolation appears to suppress the gas−liquid transition under the conditions of interest here, where the chaining interaction is stronger than the junction-forming interaction.

**B. Comparison of Theory and Simulation.** Grand canonical (constant $\mu VT$) Monte Carlo simulations were performed to test the mean-field theory and, in particular, to determine whether chain flexibility (which enters the theory only through its contribution to the chain and junction association constants) affects the thermodynamics of the transition. Two model systems were used, one "semiflexible" with chain persistence length $l_p = 10$ (in units of bond length) and another "flexible" ($l_p \approx 4$). Association constants for chaining and junction formation were matched, as shown in Table 1, so as to isolate the effects of flexibility. Isotherms showing the dependence of chemical potential on density were obtained from simulations performed over a range of values of $\mu$ (Figure 3). The plateau discontinuities at the three lower temperatures of the semiflexible system indicate coexistence regions; these discontinuities are absent in all four isotherms of the flexible system, suggesting a significant role of persistence length not accounted for in the mean-field theory. The gas−liquid transitions observed in the semiflexible system will first be addressed, followed by a discussion of their absence in the flexible system.

The $\mu$-$\varphi$ isotherms of the semiflexible system shown in Figure 3 indicate a re-entrant phase transition, with an upper critical point above $T = 0.121$ and a coexistence region that narrows as temperature is lowered, in qualitative agreement with the mean-field results and Figure 1. Inspection of simulation snapshots of the system on either side of the transition, examples of which are shown in Figure 4, confirms that the low-density or gas phase consists of disconnected chains and clusters of joined chains, whereas the higher density phase has a percolated network structure. Use of parameters from the simulation (Table 1) into the theory does not, however, give a good correspondence between the two. The upper bound to the phase transition observed in the simulation is not reproduced by the theory, which instead predicts a very broad gas−liquid transition in which the average chain lengths of both phases are near one, up to significantly higher temperatures. Unlike the simulation, in which a junction can only form at the interior of a chain, the present theory counts all monomers (including chain ends, free monomers, and existing junctions) in the system as potential junction sites. Comparisons between simulation and theory (in its current state) can only therefore be valid in the long-chain limit. This limit is not approached except perhaps at the lowest temperature point, where mean chain length $M > 20$ in the coexisting phases (Figure 5). Another qualitative discrepancy

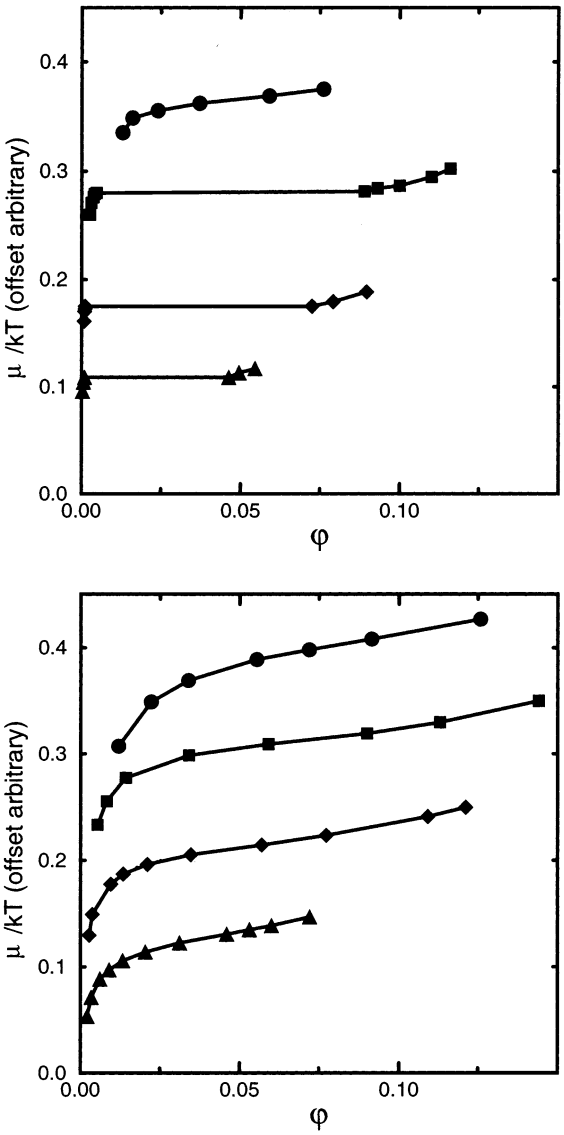


**Figure 3.** Isotherms from grand canonical Monte Carlo simulations. Upper panel: semiflexible model, $\theta_{min} = 2.5$. Lower panel: flexible model, $\theta_{min} = \pi/2$. Circles: $k_BT = 0.167$; squares: $k_BT = 0.121$; diamonds: $k_BT = 0.094$; triangles: $k_BT = 0.078$. Simulation conditions are as presented in Table 1.

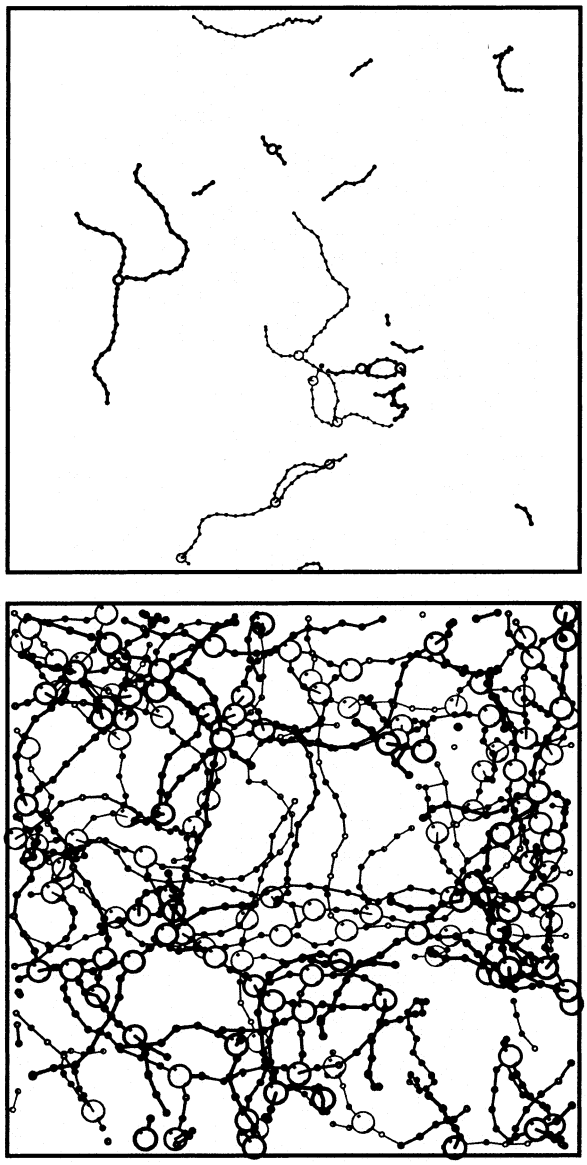

**Figure 4.** Snapshots of coexisting phases from grand canonical Monte Carlo simulations of semiflexible system at $k_BT = 0.12$. Junctions are indicated by large circles. Upper panel: gas phase, $\varphi = 0.001$, box edge length = 60. Lower panel: network phase, $\varphi = 0.07$, box edge length = 25.

between theory and simulation is seen in the change in mean chain length across the observed gas−liquid transition. While the theory predicts a negligible change, in both middle temperature points of the semiflexible chain/network simulation, the mean chain length increases by roughly 35%. This increase is only 5% at the lowest temperature point. During formation of a network of shorter chains (chain lengths 6−15), repulsions between junction sites (which, within the simulation model, must be spaced at least two monomers apart on a chain) may drive up the average chain length (providing more potential sites for fewer junctions) compared to the ideal case described by the theory.

**C. Flexible Chains: The Role of Loops.** The flexible system shows a much greater discrepancy between theory and simulation in that no phase coexistence region was observed at any temperature investigated. The ratio of junctions to chain ends, presented in Figure 6 for both flexible and semiflexible systems, is predicted by the mean-field theory to rise from a value less than one to a value greater than one across the coexistence region, as a gas of mostly free chains assembles into a network with most chains ending in junctions. This holds for all three transitions observed in the semiflexible system. For the system of flexible chains, however, the junction/end ratio exceeds unity even under dilute conditions. The "sticky" chain ends whose attractions for chain interiors give rise to the phase transition are missing, along with the transition itself.

The high number of junctions formed by flexible chains under dilute conditions can be attributed to the formation of loops. In the dilute limit, most junctions are intrachain junctions formed when a chain end loops back to bond with a monomer in the interior of the same chain. A network still is formed as the volume fraction increases and interchain junctions compete with loops; however, the energy released by formation of a network is small, because intrachain junctions must be broken for interchain junctions to be formed. The competition between inter- and intrachain junction formation is evident when the ratio of loops to total number of junctions is plotted as a function of concentration (Figure 7). The decrease in the loop fraction represents the increase in interchain junctions and a continuous

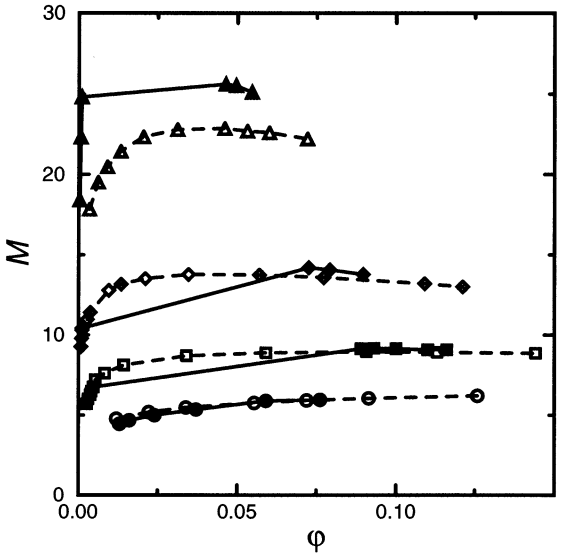


**Figure 5.** Mean chain length $M$ from Monte Carlo simulations. Solid lines/filled symbols: semiflexible model, $\theta_{min} = 2.5$. Dashed lines/open symbols: flexible model, $\theta_{min} = \pi/2$. Symbols are as in Figure 3.

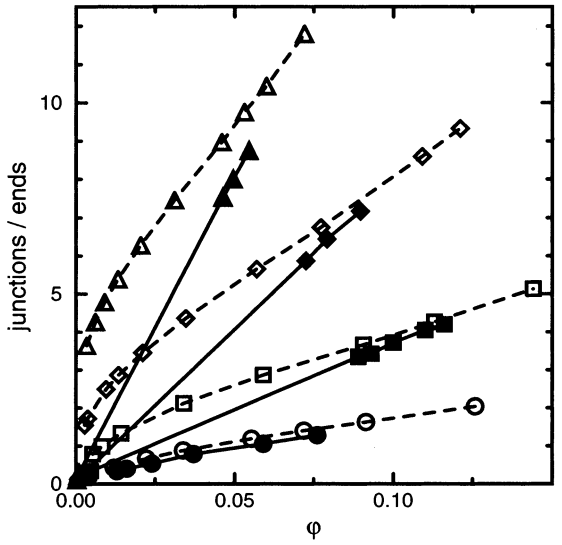


**Figure 6.** Ratio of average number of junctions to average number of free chain ends from Monte Carlo simulations. Solid curves/filled symbols: semiflexible model, $\theta_{min} = 2.5$. Dashed curves/open symbols: flexible model, $\theta_{min} = \pi/2$. Symbols are as in Figure 3.

progression into a network. The resulting curves are fit to a first approximation by the functional form

$$\frac{N_{loops}}{N_{junctions}} = \frac{\varphi_{intra}}{\varphi + \varphi_{intra}} \tag{29}$$

where $\varphi$ is the mean-field (total) concentration of monomers and $\varphi_{intra}$ is the average local effective concentration of loop-forming sites. The best-fit values of $\varphi_{intra}$ were found to be 0.0030, 0.0061, and 0.013 in order of decreasing temperature. The dependence of $\varphi_{intra}$ on temperature is related to increasing chain length upon cooling. (In the present model, chain flexibility is does not depend on temperature.) An independent, general approximation to $\varphi_{intra}$ as a function of chainlength and flexibility can be obtained using the analytic results of Shimada and Yamakawa,[22] who calculated the probability that a persistent wormlike chain will have its ends close to each other, averaged over all relative orientations of the ends, in the short and long

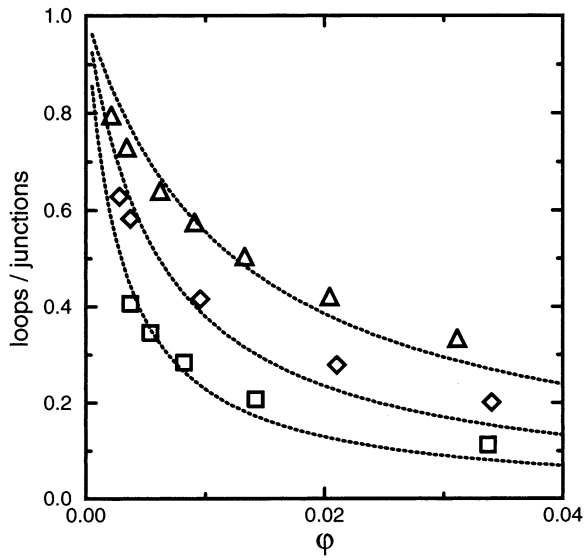


**Figure 7.** Ratio of average number of loops to average number of junctions from Monte Carlo simulations of flexible model. Dotted curves are least-squares fits to $\varphi_{intra}/(\varphi_{intra} + \varphi)$, with $\varphi_{intra} = 0.0030$ ($k_BT = 0.121$, squares); $\varphi_{intra} = 0.0061$ ($k_BT = 0.094$, diamonds); $\varphi_{intra}$=0.013 ($k_BT = 0.078$, triangles).

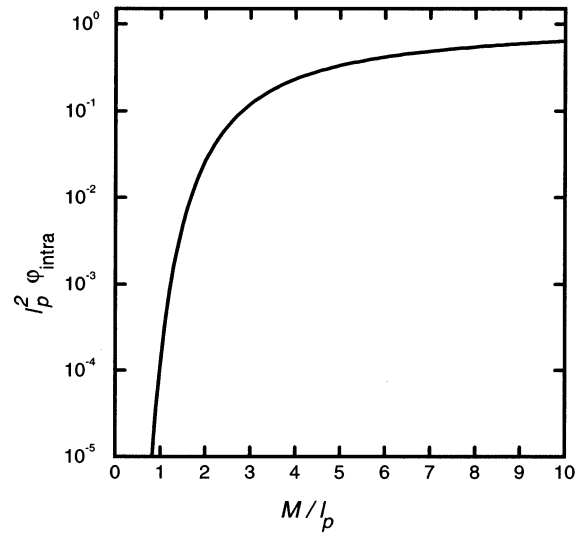


**Figure 8.** Effective concentration of intrachain junctions sites $\varphi_{intra}$ versus chainlength $M$ for wormlike polymer of persistence length $l_p$, calculated by integration of eq 30, taken from ref 22.

chain limits

$$J_{loop,small\ L} = 16\pi \times 28.01L^{-5} \exp(-14.054L^{-1} + 0.246L)$$

$$J_{loop,large\ L} = 4\pi \times (\pi L/3)^{-3/2}\left(1 - \frac{5}{4L} - \frac{79}{160L^2}\right) \tag{30}$$

where $L$ is the contour length in units of the persistence length, $l_p$, and the result is in units of $l_p^{-3}$. The integral of $J_{loop}$ over chainlengths up to $M$ is required for the calculation of $\varphi_{intra}$, to take into account the possibility of intrachain junctions formed all along the length of the chain. The functions were joined at their crossing point ($L = 9.9$, at which they are nearly parallel) and integrated numerically to yield the function graphed in Figure 8. For average chain lengths less than one persistence length, the probability of loop formation is naturally very low. Within the noninteracting chain approximation, the function approaches a constant value near 1.4 $l_p^{-2}$ in the limit of long

chains, but only very slowly, as $M^{-1/2}$. There are numerous effects not incorporated into the function, including all excluded volume effects, and even if they were included the probability of a loop forming from two chain ends differs from the probability of a loop of the same size forming from a chain end and an interior segment.[23] The probability of forming the second loop on a chain, moreover, is certainly different than that of forming the first. The polydispersity of the self-assembled system is yet another complication. The function in Figure 8 can provide a useful estimate, however, of whether a system of interest is in the regime where loop formation will compete significantly with intrachain junction formation.

Using the effective intrachain concentration as a correction to the mean concentration allows loop formation to be introduced the mean-field theory

$$f_{jn}(\varphi,T,M) = f_{ch} - 2kT\frac{\varphi}{M}\ln[1 + [\varphi + \varphi_{intra}(M)]\exp(\beta U_j^*)] \quad (31)$$

For the present purpose of demonstrating that loop formation may suppress the coexistence region, as it appears to do in the simulated flexible system, a cruder but much more convenient approximation will serve, in which $\varphi_{intra}$ is independent of $M$. Phase coexistence regions are shown in Figure 1 for several values of this constant $\varphi_{intra}$; at $\varphi_{intra} > 0.015$, no coexistence is seen. These results suggest that if loop formation is competitive with interchain clustering near the region in which mean-field theory predicts a gas−liquid transition, that transition may be suppressed.

Beyond the possibility of forming one or two intrachain loops per chain, the possibility of intra*cluster* loops also raises the effective volume fraction for junction formation beyond the mean, likewise contributing to the suppression of the gas−liquid transition. This effect may be viewed in terms of a surface energy. The number of free ends in any aggregate, multiplied by the free energy of junction formation, constitutes the surface energy that may be released through interactions with other aggregates. The capability of free ends in a cluster of flexible chains to loop back and attach to a monomer on the cluster lowers the surface energy and reduces the driving force to condense. The analysis of multichain loops, both within the simulation and the theory, is quite involved and was not attempted.

Ring formation, or the end-end bonding of a single chain, was not considered in the theory nor permitted in the simulations. It may play an important role at low volume fraction and high bonding energy in flexible systems, and has been studied by theory[24] and by simulation using models of short-ranged bonding[25] as well as dipolar interactions.[12] The ring-chain equilibrium, like the loop-chain equilibrium, probably tends to suppress the gas−liquid transition in this type of system by reducing the concentration of available ends.

A previous theoretical investigation by Drye and Cates[26] of the effect of flexibility on the thermodynamics of a network of self-assembled chains came in fact to a prediction contrary to that observed in the present simulations, i.e., that the flexible chain network but not a rigid chain system would coexist with a dilute phase. The considerations in that study were very different; the differences in excluded volume interactions between flexible chains and rigid rods were primary considerations, and the presence of free ends in the concentrated phase was neglected entirely.

Direct evidence of networks,[27] as well as both loops (referred to as "lassos") and rings,[28] formed from wormlike micelles of dimeric and tetrameric surfactants has been captured recently by cryo-transmission electron microscopy. These results offer the opportunity to refine the input parameters to theory and simulation—fundamental properties such as end energy, persistence length, and junction energy may be estimated from a distribution of ring and loop sizes under a single set of conditions[28]—and to test the predictions against results at other conditions.

## IV. Concluding Remarks

The statistical thermodynamics of a network of self-assembled chains connected by 3-fold junctions has been re-derived using an approach complementary to that of Tlusty and Safran. A benefit of the new approach, which treats junctions in terms of an equilibrium binding of a chain end to a chain interior site, is that the average chain length remains approximately constant across the gas−liquid transition. The transition can therefore easily be interpreted as a condensation of chains of a fixed size distribution, driven by the energy of junction formation. Monte Carlo simulations of a model self-assembling system of chains and junctions were performed to test the theory's predictions and to determine the effects of chain flexibility on the phase transition. A reentrant gas−liquid transition, qualitatively similar to the theoretical predictions, was observed when chains were made semiflexible ($l_p = 10$) but not for a more flexible model. This difference appears to be the product of loop or intrachain junction formation, which competes with network formation and lowers the energetic driving force of the transition. Independent estimates of the regime in which loop formation is prevalent were obtained, and a crude correction accounting for loop effects was introduced into the mean-field theory and shown to suppress the gas−liquid transition.

The influence of rings (loops joined at the end, with no 3-fold junction) on the presence of the gas−liquid transition will be one direction for further study. A recently developed Monte Carlo method will be useful in simulations of self-assembled systems rich in rings.[29] Another topic of interest, proposed[11,30] to be of importance in the sol−gel transition of actin,[31] is the competition between nematic ordering and network formation. This will require investigation of systems at higher persistence length and/or higher density than in the current conditions, at which no nematic ordering was observed in the presence or absence of junctions. Finally, the present Monte Carlo methods are inefficient for the simulation of networks with a very low concentration of free ends. Implementation of a fixed-endpoint chain re-growth algorithm to change the positions of junctions would be a way to address this limitation and examine the structural properties of equilibrium networks well above the percolation transition, where interesting effects have been predicted.[11]

**Acknowledgment.** I thank A. Zilman for invaluable discussions, and for access to the unpublished work of Zilman and Safran. Acknowledgment is made to the Cherry L. Emerson Center of Emory University, which is supported in part by a National Science Foundation grant (CHE-0079627) and an IBM Shared University Research Award, for the use of its resources. The author is a Camille and Henry Dreyfus New Faculty Awardee.

## References and Notes

(1) Gelbart, W. M.; Ben-Shaul, A. *J. Phys. Chem.* **1996**, *100*, 13 169.
(2) Israelachvili, J. N.; Mitchell, D. J.; Ninham, B. W. *J. Chem. Soc., Faraday Trans. 1* **1976**, *72*, 1525.
(3) Tlusty, T.; Safran, S. A. *Science* **2000**, *290*, 1328.

(4) Camp, P. J.; Shelley, J. C.; Patey, G. N. *Phys. Rev. Lett.* **2000**, *84*, 115.
(5) de Gennes, P. G.; Pincus, P. A. *Phys. Kond. Mater*. **1970**, *11*, 189.
(6) Tavares, J. M.; Telo da Gama, M. M.; Osipov, M. A. *Phys. Rev. E* **1997**, *56*, R6252.
(7) van Leeuwen, M. E.; Smit, B. *Phys. Rev. Lett.* **1993**, *71*, 3991.
(8) Kalikmanov, V. *Physica (Amsterdam)* **1992**, *183A*, 25; Wertheim, M. *J. Chem. Phys.* **1971**, *55*, 4291; Rushbrooke, G.; Stell, G.; Hoye, J. *Mol. Phys.* **1973**, *26*, 1199.
(9) Sear, R. P. *Phys. Rev. Lett.* **1996**, *76*, 2310; Levin, Y. *Phys. Rev. Lett.* **1999**, *83*, 1159.
(10) Tlusty, T.; Safran, S. A.; Menes, R.; Strey, R. *Phys. Rev. Lett.* **1997**, *78*, 2616; Tlusty, T.; Safran, S. A.; Strey, R. *Phys. Rev. Lett.***2000**, *84*, 1244.
(11) Zilman, A.; Safran, S. A. arXiv:cond-mat/0205488, submitted to *Phys. Rev. E.*
(12) Camp, P. J.; Patey, G. N. *Phys. Rev. E* **2000**, *62*, 5403.
(13) Kumar, S. K.; Douglas, J. F. *Phys. Rev. Lett.* **2001**, *8718*, 8301.
(14) Gilra, N.; Cohen, C.; Panagiotopoulos, A. Z. *J. Chem. Phys.* **2000**, *112*, 6910.
(15) Duda, Y.; Segura, C. J.; Vakarin, E.; Holovko, M. F.; Chapman, W. G. *J. Chem. Phys.* **1998**, *108*, 9168.
(16) Busch, N. A.; Wertheim, M. S.; Yarmush, M. L. *J. Chem. Phys.***1996**, *104*, 3962.; Wierzchowski, S.; Kofke, D. *ibid.* **2001**, *114*, 8752.
(17) Kindt, J. T.; Gelbart, W. M. *J. Chem. Phys.* **2001**, *114*, 1432.
(18) Hill, T. P. *An Introduction to Statistical Thermodynamics*; Dover: New York, 1986.
(19) McQuarrie, D. A. *Statistical Thermodynamics*; University Science Books: Mill Valley, CA, 1973.
(20) Frenkel, D.; Smit, B. *Understanding Molecular Simulation*; Academic Press: San Diego, 1996.
(21) Ferrenberg, A. M.; Swendsen, R. H. *Phys. Rev. Lett.* **1988**, *61*, 2635; Ferrenberg, A. M.; Swendsen, R. H. *Phys. Rev. Lett.* **1989**, *63*, 1195.
(22) Shimada, Y.; Yamakawa, H. *Macromolecules*, **1984**, *17*, 689.
(23) Chan, H. S.; Dill, K. A. *J. Chem. Phys.* **1990**, *92*, 3118.
(24) van der Shoot, P.; Wittmer, J. P. *Macromol. Theory Simul.* **1999**, *8*, 428.
(25) Wittmer, J. P.; van der Schoot, P.; Milchev, A.; Barrat, J. L. *J. Chem. Phys.* **2000**, *113*, 6992.
(26) Drye, T. J.; Cates, M. E. *J. Chem. Phys.* **1992**, *96*, 1367.
(27) Bernheim-Groswasser, A.; Zana, R.; Talmon, Y. *J. Phys. Chem. B* **2000**, *104*, 4005.; Bernheim-Groswasser, A.; Zana, R.; Talmon, Y. 12 192.
(28) In, M.; Aguerre-Chariol, O.; Zana, R. *J. Phys. Chem. B* **1999**, *103*, 7747.
(29) Kindt, J. T. *J Chem. Phys.* **2002**, *116*, 6817.
(30) Borukhov, I.; Bruinsma, R. F. *Phys. Rev. Lett.* **2001**, *8715*, 8101.
(31) Tempel, M.; Isenberg, G.; Sackmann E. *Phys. Rev. E* **1996**, *54*, 1802.